

## Scaling of inner and outer regions for flat plate boundary layers

R. Mathis, N. Hutchins and I. Marusic

Department of Mechanical Engineering  
University of Melbourne, Victoria, 3010 Australia

### Abstract

A new view of the scaling of the streamwise turbulence intensity profile is proposed for the zero pressure gradient turbulent boundary layer. The method is based on the scale decomposed streamwise velocity component, separated into a small- and a large-scale contribution using a wavelength pass-filter. This enables us to understand how large and small scale motions affect the streamwise turbulence intensity profile. It is found that the small-scale energetic content collapses remarkably well over a large range of Reynolds number ( $2800 \leq Re_\tau \leq 19000$ ). On the other hand, the large-scale energetic content does not simply collapse in inner, outer or mixed scaling, but a clear peak emerges, which corresponds with the location of the spectral outer-peak. The peak location appears to follow the middle of the logarithmic layer, as well as the zero amplitude modulation location described by Mathis *et al.* [8]. The intensity of the outer-peak is found to grow much more rapidly than the inner-peak, as the Reynolds number increases, possibly supporting the controversial conjecture that at sufficient high Reynolds number, the outer-peak may overcome the inner-peak. Finally, this approach allows us to explore new scaling parameters for the streamwise turbulence intensity, potentially leading to more accurate formulation in flat-plate boundary layers.

### Introduction

Over the past decade or so, the Reynolds number scaling of the zero pressure gradient turbulent boundary layer has attracted numerous studies [2, 11, 6, and others]. Despite these efforts, significant questions remain open to debate. Whilst the mean flow is generally accepted to follow the law of the wall, the scaling of the Reynolds stresses and higher moments such as skewness and flatness remain unclear. The streamwise broadband-turbulence intensity  $u^2$ , the easiest component of the Reynolds stresses to measure, has received most of the attention. It is now well established that  $\overline{u^2}$ , represented in inner variables, is Reynolds number dependent. However, these so-called Reynolds number effects remain exclusively empirically described, and a lack of theory to support it remains. Furthermore, questions regarding the applicability of inner and outer scaling regions remain and is perhaps the greatest point of contention in scaling analysis. Nevertheless, recent investigations performed in novel high Reynolds number facilities have provided more insight about the Reynolds number effects. Indeed, it has been observed that these effects are strongly correlated to the increasing large-scale energy content arising from strengthening of the large-scale motions associated with the log-layer [3, 8, 7]. However, these observations remain largely qualitative and the associated contribution of small- and large-scale motions is unclear. This paper proposes a new view of the scaling of the streamwise turbulence intensity with Reynolds number. The underlying idea is that the streamwise velocity component can be decomposed into a small- and a large-scale contribution using a wavelength pass-filter, respectively below and above a carefully selected cutoff length scale  $\lambda_x^+ = 7000$  [4, 8]. The friction Reynolds number or Kármán number is defined as  $Re_\tau = \delta U_\tau / \nu$ , with  $\delta$  the boundary layer thickness,  $U_\tau$  the friction

velocity and  $\nu$  the kinematic viscosity. Over-bars indicate time-averaged values and the superscript '+' is used to denote viscous scaling of length  $z^+ = zU_\tau/\nu$ , velocities  $u^+ = u/U_\tau$  and wavelength  $\lambda_x^+ = \lambda_x U_\tau/\nu$ . The inner and outer scaling mentioned above refer to the regions where the intensity can be collapsed respectively in inner variables  $\overline{u^{+2}} = f(z^+)$  and in outer variables  $\overline{u^{+2}} = g(z/\delta)$ .

### Experimental data-set

To investigate the Reynolds number scaling of the streamwise turbulence intensity profile, an experimental data-set obtained from zero pressure gradient turbulent boundary layer is used. The setup and detailed results have been previously described in Refs. [5] and [8]. For consistency, we will briefly recall some of the boundary layer properties along with the main measurements characteristics.

Measurements were made in the large boundary layer wind tunnel at the University of Melbourne. This facility – also known as HRNBLWT (High Reynolds Number Boundary Layer Wind Tunnel) – consists of an open-return blower with a working test section of  $27 \times 2 \times 1$  m, and a low free-stream turbulence intensity, nominally 0.05%. A zero pressure gradient is maintained along the working test section by bleeding air from the tunnel ceiling through adjustable slots. Further details of the facility can be found in Ref. [13]. Data considered here were obtained between  $x = 5$  and  $x = 21$  m downstream of the tripped inlet, over the range  $Re_\tau = 2800$  to 19000. The full details of the experimental conditions are given in table 1.

All measurements were carried out using hot-wire anemometry. To avoid the complication of spatial resolution problems (a recurrent issue in near-wall turbulence measurements, see Ref. [5]), a constant viscous scaled wire length,  $l^+ = 22$ , and a ratio  $l/d \geq 200$  have been used for all Reynolds numbers. This setup allows us to have a reasonably small amount of attenuation of the turbulent kinematic energy (see Refs [5] and [1] for further details about spatial resolution effects and possible correction methods). The frequency and sampling duration have been carefully chosen to allow capture of the small-scale energy content as well as fully converged large-scale motions (table 1).

### Results and discussion

Figure 1a shows the total streamwise turbulence intensity profile over the large range of Reynolds number experiments performed in the Melbourne wind tunnel. As expected, the inner-peak  $\overline{u^{+2}}(z^+ = 15)$  shows a Reynolds number dependence, characterised by a weak rise of the peak intensity. The slope of the logarithmic trend of the inner-peak remains debatable, due to non uniform  $l^+$  in measurements available in the literature. Considering only our data, the peak intensity follows the logarithmic evolution  $0.39 \ln Re_\tau + 4.8$ , whereas Hutchins and Marusic [3, Fig. 8] proposed  $0.69 \ln Re_\tau + 2.65$ . Discrepancy between these formulations (and many others in the literature) is strongly dependent of the set of data chosen. Hutchins and Marusic [3, Fig. 8] incorporated in their analysis a large set of data covering four orders of magnitude in Reynolds number, but with large disparity in  $l^+$ . Here, we chose to use a restricted set of data,

$Re_\tau$	$x$ (m)	$U_\infty$ (m/s)	$\delta$ (m)	$U_\tau$ (m/s)	$\nu/U_\tau$ ( $\mu\text{m}$ )	$l^+$	$l/d$	$\Delta T^+$	$TU_\infty/\delta$
2800	5	11.97	0.098	0.442	35.0	22	200	0.53	14600
3900	8	11.87	0.140	0.426	36.0	21	200	0.49	15200
7350	21	10.30	0.319	0.330	44.0	23	200	0.34	17400
13600	21	20.54	0.315	0.671	23.0	22	200	0.48	15700
19000	21	30.20	0.303	0.960	16.0	22	233	0.59	12000

Table 1: Experimental parameters for hot-wire measurements, where  $U_\infty$  is the free-stream velocity,  $l$  the etched length of the hot-wire,  $d$  its diameter, and  $\Delta T^+$  and  $T$  the frequency and sampling duration respectively.

covering ‘only’ one order of magnitude, but with a consistent  $l^+$  so that error in logarithmic slope would be minimised. Indeed, the attenuation of the peak intensity due to spatial resolution issues was shown by Chin *et al.* [1] to be only dependant on  $l^+$ , not on  $Re_\tau$ . Therefore, the small amount of attenuation in our measurements should not affect the logarithmic trend, but may affect the additive constant.

#### Scale decomposition

As mentioned above, Reynolds number effects have been related to the large-scale energy content, which increases with Reynolds number. The underlying assumption of such a hypothesis, is that the small-scale energy content will remain the same at all  $Re_\tau$ , and so the increasing energy in the  $\overline{u^{+2}}$  profile with increasing  $Re_\tau$  should correspond to the strengthening con-

tribution from the large-scale motions. To understand further how large and small scale motions affect the streamwise turbulence intensity, we decompose  $\overline{u^{+2}}$  into a small-  $\overline{u_S^{+2}}$  and a large-scale  $\overline{u_L^{+2}}$  component, such that  $\overline{u^{+2}} = \overline{u_S^{+2}} + \overline{u_L^{+2}}$ . To achieve such a decomposition, the fluctuating  $u^+$  signal was first separated into a short-wavelength content signal  $u_S^+$  (where  $\lambda_x^+ < 7000$ ) and a long-wavelength content signal  $u_L^+$  (where  $\lambda_x^+ > 7000$ ). Then  $\overline{u_S^{+2}}$  and  $\overline{u_L^{+2}}$  are calculated individually on each corresponding part, respectively  $u_S^+$  and  $u_L^+$ . The choice of the cut-off wavelength was carefully made according to the pre-multiplied energy spectra maps. It was previously shown in Ref. [8, figure 1b] that  $\lambda_x^+ \simeq 7000$  seems to be a reasonable length to separate small and large scale motions. Further details of the effect of the choice of the cut-off wavelength will be given in the last section of the paper. It should be noted that such scale decomposition remains valuable due to a sufficient separation between the inner and outer length scales. Hutchins and Marusic [4, 3] show that a minimum  $Re_\tau \simeq 2000$  is necessary to ensure a good scale separation (or at least to see emergence of large-scale motions in the energy spectra). Figure 1b shows the broadband intensity profiles decomposed into small- (solid lines) and large-scale (dashed lines) components. The summation of both components is equal to the total contribution shown in figure 1a. Clearly, the small scale energy content, which accounts for the majority of the near-wall peak, collapses well in inner-scale  $z^+$  for all  $Re_\tau$ . The large-scale content appears to principally contribute to the log-region, but a significant portion of energy remains close to the wall, contributing to the slight increase of the near-wall peak. This supports the assumption that the Reynolds number effects are closely related to the large-scale motions.

#### Large-scale energy content

Interestingly, the scale decomposition employed here highlights a clear peak in the large scale component  $\overline{u_L^{+2}}$  (filled-circles in figure 1b). Therefore it is logical to consider whether or not this peak corresponds to the signature of the superstructure type events [3], as observed in the pre-multiplied energy spectra maps [8, 7], usually referred to as the spectral outer-peak. To understand further the significance of the peak in the large-scale component  $\overline{u_L^{+2}}$ , we can study the Reynolds number trend of its location as well as of its intensity. To accurately locate the peak, the  $\overline{u_L^{+2}}$  profiles in figure 1b (dashed lines) were fitted using a six order polynomial function. Indeed, even with a sampling length in the range of 12000 to 17000 boundary turn overs, the large-scale energy content appears to be not fully converged, and residual noise is still visible on the  $\overline{u_L^{+2}}$  profiles (which could alter the results). The Reynolds number evolution of the wall-normal location and turbulence intensity of  $\overline{u_L^{+2}}$  are shown in figures 2a and 2b, respectively. Also shown in figure 2a is the location where the degree of amplitude modulation crosses zero (square symbols) and the slope of the middle of the

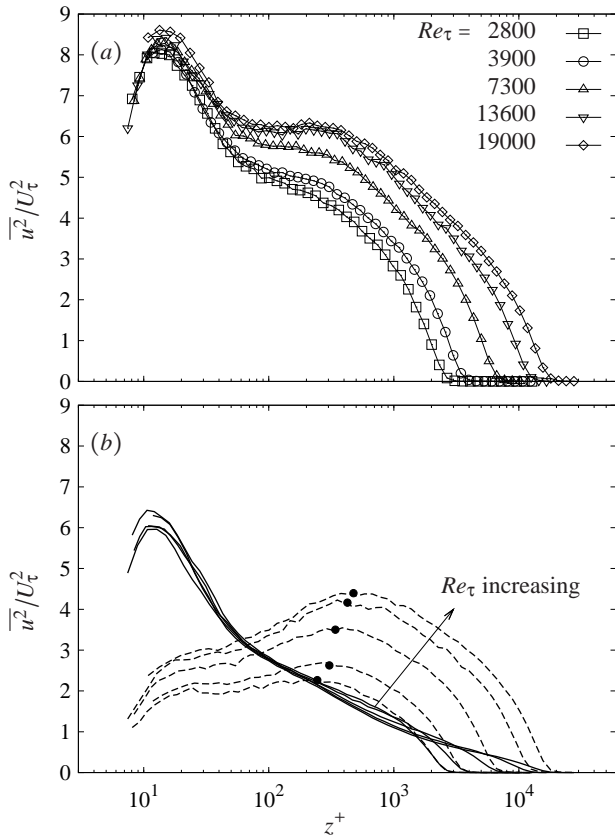


Figure 1: (a) Reynolds number dependency of the streamwise turbulence intensity profiles  $\overline{u^2}/U_\tau^2$ ; (b) Decomposition of the streamwise turbulence intensity profile into small-scale ( $\lambda_x^+ < 7000$ , solid lines) and large-scale components ( $\lambda_x^+ > 7000$ , dashed lines), the sum of both components is equal to profiles in figure (a).

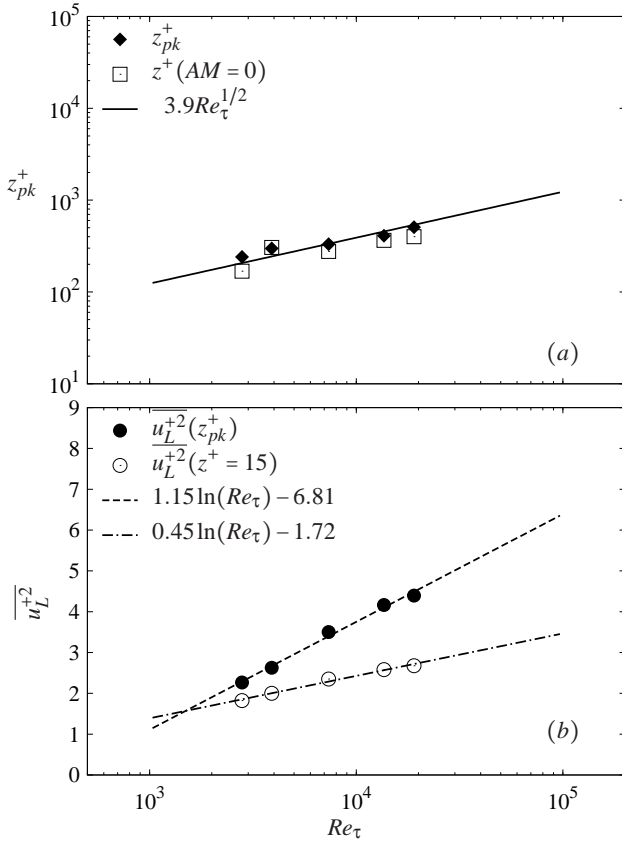


Figure 2: Reynolds number dependency of (a) the wall-normal location  $z_{pk}^+$  of the peak in the profile of the large-scale component of the streamwise turbulence intensity ( $\square$ ), with the location where the degree of amplitude modulation crosses zero ( $\blacklozenge$ ), and the slope of the centre of the log-region (solid line); (b) the turbulence intensity of the large-scale component at the inner- ( $\circ$ ) and outer-peak ( $\bullet$ ) locations; The dotted-dashed line and the dashed line are the respective log-law curve fits.

log-layer  $3.9Re_\tau^{1/2}$  (solid line) as given by Ref. [8].

The large-scale peak location  $z_{pk}^+$  is found to collapse well with the location of zero amplitude modulation and the  $3.9Re_\tau^{1/2}$  slope, which was shown by Mathis *et al.* [8] to match the location of the outer-peak on pre-multiplied energy spectra maps. Therefore, the  $\overline{u_L^{+2}}$  peak seems to describe well the location of the outer-peak, and the scale decomposition applied here to the streamwise turbulence intensity profile appears to be a robust method to localise this outer-peak (further details about the cut-off effects are given hereafter).

Interesting features can be interpreted from the Reynolds number trend of the large-scale peak given in figure 2b (filled-circles) along with the large-scale intensity trend at the near-wall peak  $\overline{u_L^{+2}}(z^+ = 15)$  (open-circles), both following a logarithmic evolution. It is interesting to note that the large-scale energy content at the inner-peak location (open-circle) increases at a rate very close to the total inner-peak energy ( $0.39 \ln(Re_\tau)$ ). This is in good agreement with previous studies showing that the additional energy in the near-wall streamwise fluctuation comes from low-wavenumber events [11]. On the other hand, the large-scale energy content at the outer-peak  $\overline{u_L^{+2}}(z_{pk}^+)$  is found to grow three times faster, as  $Re_\tau$  increases, than at the inner-peak. These trends, shown in figure 2b, indicate that at a sufficiently high Reynolds number the streamwise turbulence energy content at the outer-peak will overcome the near-wall

peak in the total streamwise turbulence energy profile. The extrapolated result in figure 3 indicates such behaviour may occur around  $Re_\tau = 10^7$ . Such questions remain controversial [12, 10, 7], and it is noted that accurate near-wall measurements face considerable challenges (thus there could be some residual error in the open circle data of figure 2b and 3). Further data at high Reynolds number and with minimal spatial and temporal resolution effects are needed to fully resolve this. However, such scale decomposition presented here gives some first clues to further understand such Reynolds number effects.

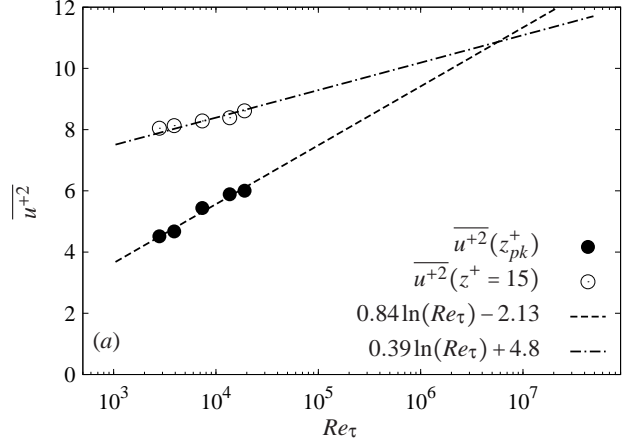


Figure 3: Reynolds number dependency of the total streamwise turbulence intensity at the inner- ( $\circ$ ) and outer-peak ( $\bullet$ ) locations; The dotted-dashed line and the dashed line are the respective log-law curve fits.

#### New scaling view

If the small-scale component  $\overline{u_S^{+2}}$  appears to collapse well using inner-scales  $z^+$  and  $U\tau$ , it would be valuable – for streamwise turbulence intensity formulation purposes – to also collapse the large scale component  $\overline{u_L^{+2}}$  on appropriate scaling. Unfortunately, no scaling variables have yet been found to fulfil this. One of the issues resides in the fact that the outer-peak location and its turbulence intensity are Reynolds number dependant. However, for future consideration it is interesting to present here the set of variables tested: for the wall-normal location,  $z^+$ ,  $z/\delta$  and  $z^+/z_{pk}^+$  have been tested, whereas for the turbulence intensity,  $U_\tau^2$ ,  $U_\infty^2$ ,  $U_\infty U_\tau$ ,  $U^2(z_{pk}^+)$ ,  $U(z_{pk}^+)U_\infty$  and  $U(z_{pk}^+)U_\tau$ , have been tried.

Nevertheless, by applying the same set of variables to the streamwise turbulence intensity profile, some interesting collapse of the profile in the log-region appeared using the outer-peak location  $z_{pk}^+$  and its corresponding mean local velocity  $U^2(z_{pk}^+)$ . In figure 4, a remarkable collapse is observed in the log-region, where  $z^+/z_{pk}^+ = 1$  denotes the mid-point of the equilibrium logarithmic layer.

#### Cut-off wavelength effect

The results discussed above are based on a scale decomposition, and results might be dependent on the choice of the cut-off parameter. In this section, we study the effect of the location of the cut-off wavelength, ranging from  $\lambda_x^+ = 5000$  to  $\lambda_x^+ = 10000$ . For each cut-off wavelength considered, it is found that the general behaviour of both small-  $\overline{u_S^{+2}}$  and large-scale  $\overline{u_L^{+2}}$  components remain similar, as shown in figure 1b (not shown here for space reasons). Importantly, for all cut-offs a very good collapse of the small-scale energy content was observed. To gain

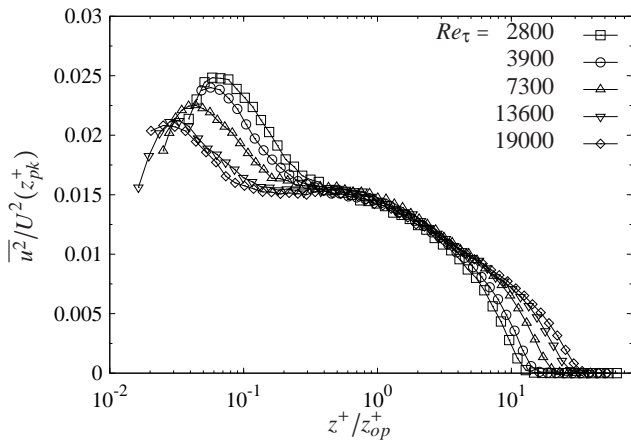


Figure 4: Scaling of the total streamwise turbulence intensity by the local mean velocity at the outer-peak  $U^2(z_{pk}^+)$  versus  $z^+/z_{op}^+$ .

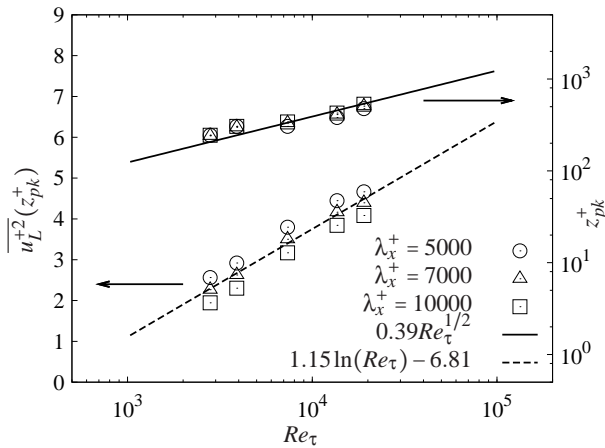


Figure 5: Effects of the cut-off wavelength on the location and intensity of the peak of the large-scale component  $u_L^{+2}$ ; The solid and dashed lines are the log-law curve fits.

a better insight into how the large-scale component is affected by the filter parameter, the peak location and intensity are reported in figure 5 for the different cases. It can be clearly seen that the peak location remains independent of the cut-off wavelength. On the other hand, the turbulence intensity peak shows a weak dependency to the cut-off, as expected, since more or less large-scale motions are taken into account by moving the cut-off wavelength. However, for all cases tested, the turbulence peak intensity follows exactly the same Reynolds number trend.

## Conclusions

A scale decomposition has been employed to study how the small- and large-scale structures influence the streamwise turbulence intensity profile. It is shown that the small-scale energetic content, when presented in inner variables, is independent of the Reynolds number, and account for the majority of the inner-peak. In contrast, the large-scale energetic motions are found to be strongly Reynolds number dependent, and contribute not only to the log-region, but all the way down to the wall. It is found that the weak rise of the inner-peak in the total energy is mainly due to the increasing large-scale activity. Furthermore, the scale decomposition, proposed here for the streamwise turbulence intensity, appears to be a reliable tool to locate the outer-peak, whose location remains debatable [8, 9]. In-

deed, it is shown that the peak in the large-scale component  $u_L^{+2}$  corresponds well with the nominal middle of the log-layer and the location of zero amplitude modulation (see Ref. [8]). More interestingly, it is observed that the outer-peak energy grows two to three times more rapidly than the inner-peak, leading to the controversial conjecture that the outer-peak energy may overcome the inner-peak content at very high Reynolds number. Finally, further research is needed in order to find variables that will collapse the large-scale component. Such scaling information would be very useful for numerical simulations that make use of formulations based on the Reynolds stress tensor.

## Acknowledgements

The authors gratefully acknowledge the financial support of the Australian Research Council.

## References

- [1] Chin, C. C., Hutchins, N., Ooi, A. S. H. and Marusic, I., Use of direct numerical simulation (DNS) data to investigate spatial resolution issues in measurements of wall-bounded turbulence, *Meas. Sci. Technol.*, **20**, 2009, 115401 (10pp).
- [2] DeGraaff, D. B. and Eaton, J. K., Reynolds number scaling of the flat-plate turbulent boundary layer, *J. Fluid Mech.*, **422**, 2000, 319–346.
- [3] Hutchins, N. and Marusic, I., Evidence of very long meandering features in the logarithmic region of turbulent boundary layers, *J. Fluid Mech.*, **579**, 2007, 1–28.
- [4] Hutchins, N. and Marusic, I., Large-scale influences in near-wall turbulence, *Phil. Trans. R. Soc. Lond. A*, **365**, 2007, 647–664.
- [5] Hutchins, N., Nickels, T., Marusic, I. and Chong, M. S., Spatial resolution issues in hot-wire anemometry, *J. Fluid Mech.*, **635**, 2009, 103–136.
- [6] Marusic, I. and Kunkel, G. J., Streamwise turbulence intensity formulation for flat-plate boundary layers, *Phys. Fluids*, **15**, 2003, 2461–2464.
- [7] Marusic, I., Mathis, R. and Hutchins, N., High Reynolds number effects in wall turbulence, *Int. J. Heat Fluid Flow*, **31**, 2010, 418–428, sixth International Symposium on Turbulence and Shear Flow Phenomena.
- [8] Mathis, R., Hutchins, N. and Marusic, I., Large-scale amplitude modulation of the small-scale structures in turbulent boundary layers, *J. Fluid Mech.*, **628**, 2009, 311–337.
- [9] McKeon, B. J. and Sharma, A. S., A critical layer framework for turbulent pipe flow, *J. Fluid Mech.*, in Press.
- [10] Metzger, M., McKeon, B. J. and Holmes, H., The near-neutral atmospheric surface layer: turbulence and non-stationarity, *Phil. Trans. R. Soc. Lond. A*, **365**, 2007, 859–876.
- [11] Metzger, M. M. and Klewicki, J. C., A comparative study of near-wall turbulence in high and low Reynolds number boundary layers, *Phys. Fluids*, **13**, 2001, 692–701.
- [12] Morrison, J., McKeon, B., Jiang, W. and Smits, A., Scaling of the streamwise velocity component in turbulent pipe flow, *J. Fluid Mech.*, **508**, 2004, 99131.
- [13] Nickels, T. B., Marusic, I., Hafez, S. and Chong, M. S., Evidence of the  $k_1^{-1}$  law in high-Reynolds number turbulent boundary layer, *Phys. Rev. Lett.*, **95**, 2005, 074501.